Combustion Theory and Modelling
Vol. 10, No. 3, June 2006, 439–458

Taylor & Francis
Taylor & Francis Group

Eulerian transported probability density function sub-filter model for large-eddy simulations of turbulent combustion

VENKATRAMANAN RAMAN*†, HEINZ PITSCH† and RODNEY O. FOX‡

†Center for Turbulence Research, Stanford University, CA 94305, USA
‡Department of Chemical Engineering, Iowa State University, IA 50010, USA

(In final form 4 November 2005)

Reactive flow simulations using large-eddy simulations (LES) require modelling of sub-filter fluctuations. Although conserved scalars like mixture fraction can be represented using a beta-function, the reactive scalar probability density function (PDF) does not follow an universal shape. A one-point one-time joint composition PDF transport equation can be used to describe the evolution of the scalar PDF. The high-dimensional nature of this PDF transport equation requires the use of a statistical ensemble of notional particles and is directly coupled to the LES flow solver. However, the large grid sizes used in LES simulations will make such Lagrangian simulations computationally intractable. Here we propose the use of a Eulerian version of the transported-PDF scheme for simulating turbulent reactive flows. The direct quadrature method of moments (DQMOM) uses scalar-type equations with appropriate source terms to evolve the sub-filter PDF in terms of a finite number of delta-functions. Each delta-peak is characterized by a location and weight that are obtained from individual transport equations. To illustrate the feasibility of the scheme, we compare the model against a particle-based Lagrangian scheme and a presumed PDF model for the evolution of the mixture fraction PDF. All these models are applied to an experimental bluff-body flame and the simulated scalar and flow fields are compared with experimental data. The DQMOM model results show good agreement with the experimental data as well as the other sub-filter models used.

Keywords: Direct quadrature method of moments; Lagrangian transported PDF; Large-eddy simulations; Flamelet; Probability density function

1. Introduction

Large-eddy simulations (LES) are being used increasingly to understand turbulent reactive flows, especially in the simulation and design of combustors. Similar interest is seen in the chemical industry where simulations can be used to optimize the performance of chemical reactors. Since chemical reactions occur predominantly at the sub-filter level, reaction models for these wide variety of applications need to take into account sub-filter fluctuations of all species in the system. The usual statistical approach to modelling scalar fluctuations requires specification of a probability density function (PDF), which in the case of LES is known as a filtered-density function [1]. A transport equation for the PDF can be formulated that spans a multidimensional solution space with derivatives in time, physical, and compositional spaces [2]. One of the key features of this equation is that the filtered reaction source term appears in

*Corresponding author. E-mail: v.raman@mail.utexas.edu

Combustion Theory and Modelling
ISSN: 1364-7830 (print), 1741-3559 (online)
http://www.tandf.co.uk/journals
DOI: 10.1080/13647830500460474

a closed form and requires no modelling. However, due to computational complexities, this transport equation is not solved directly.

There are several approaches to combustion modelling apart from the PDF approach mentioned above. In models for turbulent non-premixed combustion, reactive scalars are often parameterized using a conserved scalar like the mixture fraction. Modelling assumptions lead to a simplified system of equations for evolving reactive species. The flamelet model [3] as well as the conditional moment closure [4] fall in this category. In these models, the evolution of the reactive scalars are parameterized by a conserved scalar, namely, the mixture fraction. To compute the filtered-mean fields of the reactive scalars, the sub-filter PDF of mixture fraction is required. This is specified using the mean and sub-filter variance of mixture fraction along with a presumed-form for the PDF. Several DNS tests have shown that a beta-function reasonably approximates the shape of the PDF [5]. However, it has also been noted that the beta-function does not exactly reproduce the shape of the mixture-fraction PDF but still approximates the moments of the scalar quite accurately [6–8].

Although this simplified approach is applicable in the fast chemistry regime, parametrization using a single conserved scalar is not valid if slow reactions are of importance. Unlike the mixture fraction, the sub-filter PDF for reactive scalars cannot be specified using a beta-function. Since it is nearly impossible to determine universal functions to describe reactive scalar PDFs, the only solution is to solve for the joint-composition PDF itself. The high-dimensional nature of the PDF transport equation makes finite-differencing techniques intractable. However, this equation can be cast in the form of the well-known Fokker–Planck equation and solved using Monte Carlo methods [2, 9]. Typically, a large ensemble of notional particles is evolved in time as well as physical and compositional spaces according to a set of stochastic differential equations [1, 2, 10].

To increase the stability and computational ease of the PDF method, a hybrid approach is typically followed. Here, an external flow solver is used to provide the flow and turbulent fields. The PDF solver then advances the particles in order to evolve the scalar fields. These hybrid schemes have been successfully used for simulating several experimental configurations [11–13]. However, when the Monte Carlo method is coupled with LES solvers, such particle schemes can quickly become intractable. In this work, we will propose an Eulerian scheme, called the direct quadrature method of moments (DQMOM) for solving the PDF transport equations without having to resort to the equivalent particle system [14, 15]. The DQMOM scheme will retain all one-point statistical properties of the Lagrangian scheme. The main advantage is that it is computationally simple and can be implemented in existing filtered-scalar transport schemes with minimal effort.

In the present study, the feasibility of the DQMOM scheme for reactive flows is established. First, a simple shear-layer configuration is considered using various chemical rate-expressions. The performance of the DQMOM scheme is compared with the Lagrangian Monte Carlo scheme. Then, a bluff-body stabilized flame experiment [16] is used as test case. Several RANS-based simulations of this system using simple chemistry models have shown reasonable agreement with experimental data [17–19]. Here, we use a steady flamelet model to describe chemistry, but the sub-filter PDF of the mixture fraction is evolved using three different models. Using this test case, we will demonstrate that a simplified PDF evolution algorithm can predict the species and flow fields quite accurately. The next section details the theoretical development of the DQMOM scheme.

2. DQMOM sub-filter model for reactive flows

The joint-composition PDF in a turbulent reactive system is generally described through a one-point one-time PDF (or in LES referred to as filtered-density function), $F(\mathbf{x}, t, \psi)$ defined

such that

$$\int_{-\infty}^{\infty} F(\mathbf{x}, t, \psi) d\psi = \overline{\rho}, \tag{1}$$

$$\frac{\partial F}{\partial t} + \frac{\partial \widetilde{\mathbf{U}} F}{\partial \mathbf{x}} = \frac{\partial}{\partial \mathbf{x}} \left[\Gamma_T \frac{\partial F/\overline{\rho}}{\partial \mathbf{x}} \right] - \frac{\partial}{\partial \psi} \left[\left(\frac{1}{\bar{\rho}} \nabla \cdot \widetilde{\Gamma \nabla \phi | \psi} + \mathbf{S}(\psi) \right) F \right], \tag{2}$$

where $\widetilde{\mathbf{U}}$ is the filtered velocity field, Γ and Γ_T are the molecular and turbulent diffusivities, respectively, and $\mathbf{S}(\psi)$ is the reaction source term. Since variable density flows are considered, all filtered quantities are density weighted Favre variables except for the density. It is noted that the terms filtered-density function and probability density function are used interchangeably here.

The last term in equation (2) represents transport in composition space, and consists of mixing and reaction processes. Although the reaction source term appears closed, the molecular mixing term requires a multipoint description and is closed using a micromixing model. In spite of the wide choice of models available, none of them provides a universal closure. The mixing term is modelled here using the Interaction by Exchange with the Mean (IEM) model [20].

$$\frac{\partial}{\partial \psi} \left[\frac{1}{\overline{\rho}} \nabla \cdot \widetilde{\Gamma \nabla \phi | \psi} F \right] = -\frac{\partial}{\partial \mathbf{x}} \left(\Gamma \frac{\partial F/\overline{\rho}}{\partial \mathbf{x}} \right) + \frac{\partial}{\partial \psi} \left[\frac{1}{\tau} (\widetilde{\phi} - \psi) F \right], \tag{3}$$

where τ is a suitable turbulence time scale.

Equation (2) is commonly solved using a Lagrangian/Eulerian hybrid scheme where a particle-based Monte Carlo scheme is coupled with a flow solver [9]. To reduce the statistical errors in the simulation, a high particle number density (say $>$ 15/cell) need to be used. Three-dimensional simulations using LES flow solvers typically involve 1–10 million cells, implying that roughly 15–150 million notional particles have to be evolved. Each of these particles carry a composition vector that describes the thermochemical state of the particle. This composition vector evolves through mixing and chemical reactions. Since combustion involves stiff chemical source terms, the composition vector has to be advanced in time using computationally expensive stiff-ODE solvers. With such a large number of particles, use of even simple chemistry mechanisms will lead to very expensive simulations. In this regard, the DQMOM scheme is an alternative numerical methodology used here to solve the PDF transport equation. This method tries to overcome the computational complexity of the Lagrangian approach by formulating Eulerian transport equations for scalar quantities that will finally define the joint composition PDF itself. Unlike the particle-based method which tries to accurately resolve all moments of the PDF, the DQMOM scheme only evolves a finite-number of moments. This simplification reduces the number of partial differential equations to be solved. A schematic of the DQMOM and Lagrangian PDF decomposition is shown in figure 1. The composition-PDF describing an N_s species system is decomposed into a set of N delta-functions that are characterized by their location in composition space ($\overline{\phi}_{\alpha n}$) and the weight or height of each peak (w_n). The joint-FDF can then be written as [14]

$$P_\phi(\psi; \mathbf{x}, t) = \sum_{n=1}^{N} w_n(\mathbf{x}, t) \prod_{\alpha=1}^{N_s} \delta(\psi - \widetilde{\phi}_{\alpha n}(\mathbf{x}, t)). \tag{4}$$

This form can be directly substituted into equation (2) to obtain transport equations for the weights and locations of the peaks.

$$\frac{\partial \overline{\rho} w_n}{\partial t} + \frac{\partial \overline{\rho} \widetilde{\mathbf{U}} w_n}{\partial \mathbf{x}} = \frac{\partial}{\partial \mathbf{x}} \left[(\Gamma_T + \Gamma) \frac{\partial w_n}{\partial \mathbf{x}} \right] + \overline{\rho} a_n. \tag{5}$$

$$\frac{\partial \overline{\rho} \widetilde{G}_{\alpha n}}{\partial t} + \frac{\partial \overline{\rho} \widetilde{\mathbf{U}} \widetilde{G}_{\alpha n}}{\partial \mathbf{x}} = \frac{\partial}{\partial \mathbf{x}} \left[(\Gamma_T + \Gamma) \frac{\partial \widetilde{G}_{\alpha n}}{\partial \mathbf{x}} \right] + \overline{\rho} b_{\alpha n}, \tag{6}$$

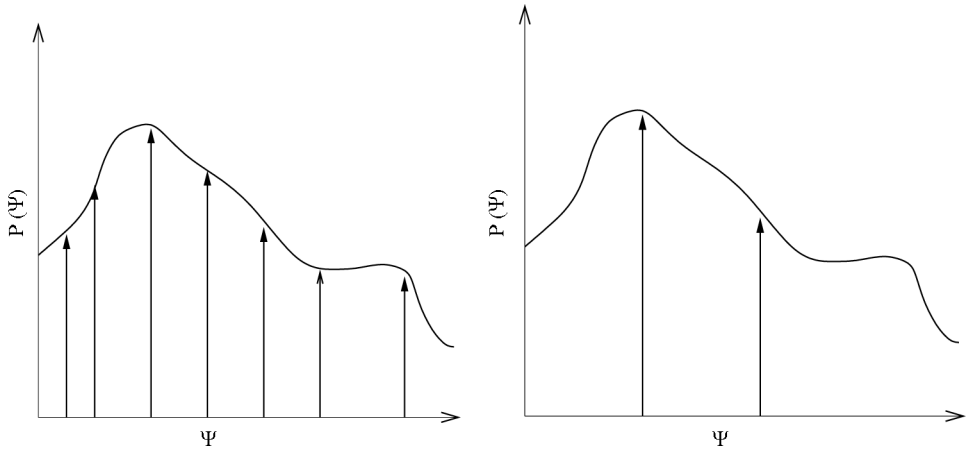

Figure 1. Approximation of a FDF using a finite number of delta-functions. (Left) Transported FDF method and (right) DQMOM method.

where $\widetilde{G}_{\alpha n} = w_n \widetilde{\phi}_{\alpha n}$. It is readily seen that these equations resemble species transport equations. Since no statistical technique is used, the numerical error in the computation is determined by the computational scheme used to discretize and advance the Eulerian equations. The level of accuracy in the compositional space can be explicitly set by choosing an appropriate number of delta-functions. The source terms for these equations (a_n and $b_{\alpha n}$) are determined by the moments of the transport term in composition space, and hence represent mixing and reaction processes.

For a single scalar case, a non-linear system can be formed to determine the source terms. The PDF transport equation is multiplied by ϕ^m and integrated over composition space to obtain a moments-based equation system [14].

$$(1-m)\sum_{n=1}^{N} \widetilde{\phi}_n^m a_n + m \sum_{n=1}^{N} \widetilde{\phi}_n^{m-1} b_n = m(m-1) \sum_{n=1}^{N} \widetilde{\phi}_n^{m-2} w_n c_n + R_m, \tag{7}$$

where c_n is defined by

$$c_n = \Gamma_T (\nabla \widetilde{\phi}_n)^2 \tag{8}$$

and R_m is the m-th moment of the mixing and reaction terms:

$$R_m = m \sum_{n=1}^{N} \overline{\rho} w_n \widetilde{\phi}_n^{m-1} \left\{ \frac{1}{\tau} (\widetilde{\phi} - \widetilde{\phi}_n) + S(\widetilde{\phi}_n) \right\}. \tag{9}$$

For a multiscalar computation, the non-linear system of equations that determines the source terms is more complex [14]. For such systems, the cross-correlations between the different species have to be evolved. However, if only the pure moments are used to specify the source terms, then all multiscalar systems will also evolve by the above set of equations. However, the covariance of the scalars can not be then controlled. One interesting feature of the DQMOM scheme is that *any* set of moments can be used to find the source terms. For example, if the first and third moments are needed to compute the reaction source terms, then $m = 1, 3$ can be used. This aspect will be particularly useful in, say, soot modelling, where the source terms may involve certain specific higher-order moments. Further details of the DQMOM approach for reacting flows can be found elsewhere [14].

Here, N is set to 2 for all simulations, although any number of delta-functions can be used. To guarantee realizability of the PDF, the source terms for the transport equation of the weight function are set to zero [14]. This simplifies the transport equations for the weights considerably. Then the non-linear system that determines the source terms for $\overline{G}_{\alpha n}$ can be written as

$$\begin{bmatrix} 1 & 1 \\ \widetilde{\phi}_1 & \widetilde{\phi}_2 \end{bmatrix} \begin{bmatrix} b_1 \\ b_2 \end{bmatrix} = \begin{bmatrix} R_1 \\ 2(w_1 c_1 + w_2 c_2) + R_2 \end{bmatrix}. \tag{10}$$

The solution of the above system along with the assumptions made lead to the following source terms:

$$a_1 = a_2 = 0, \tag{11}$$

$$b_1 = \frac{1}{\widetilde{\phi}_1 - \widetilde{\phi}_2} \sum_{n=1}^{2} w_i \Gamma_t (\nabla \widetilde{\phi}_n)^2 + \frac{1}{\tau}(w_1 \widetilde{G}_2 - w_2 \widetilde{G}_1) + w_1 S(\widetilde{\phi}_1), \tag{12}$$

and

$$b_2 = \frac{-1}{\widetilde{\phi}_1 - \widetilde{\phi}_2} \sum_{n=1}^{2} w_i \Gamma_t (\nabla \widetilde{\phi}_n)^2 - \frac{1}{\tau}(w_1 \widetilde{G}_2 - w_2 \widetilde{G}_1) + w_2 S(\widetilde{\phi}_2). \tag{13}$$

The source terms for the $\widetilde{G}_{\alpha n}$ terms contain the inverse of the distance in composition space between the delta-peaks. Numerically, this could lead to large source terms at certain locations where the sub-filter variance approaches zero. In such a scenario, the peaks will tend to approach each other leading to a singularity in the determination of the source term. In this study, this component of the source term was simply set to zero when the peaks are separated by less than a threshold value, ϵ. It was found that ϵ should be less than 10^{-3} to ensure that this approximation does not affect the results.

3. Numerical schemes

In general, the DQMOM scheme can be used with any number of delta-peaks. Wang and Fox [21] have shown that in the context of particulate formation, two delta-functions are sufficiently accurate in evolving the lower moments of the PDF. To test the accuracy of the two-peak approximation, two different flow configurations, a shear flow case and a bluff-body stabilized flame, are used. In order to estimate the effect of the DQMOM scheme on sub-filter PDF predictions, three different simulation strategies are adopted. The first simulation uses a finite-volume-based scalar transport scheme with no sub-filter models for the scalar fluctuations. The second scheme involves a transported-FDF simulation using Lagrangian particles. The third simulation was carried out with the DQMOM implementation. The shear-layer numerical experiment was designed to illustrate that the DQMOM scheme, in spite of using only a two-peak approximation provides results closer to the more detailed multipeak Lagrangian simulation, and also that neglecting sub-filter fluctuations can lead to substantial errors. The bluff-body simulations on the other hand are designed to show that in practical LES simulations, the DQMOM scheme is comparable to a presumed beta-function or a multipeak Lagrangian representation of the sub-filter FDF.

For the shear-layer configuration, a simple one-step chemistry with different rate expressions was tested. The specific functional forms of the rates were chosen to represent some of the common rate expressions used in global mechanisms. The bluff-body stabilized flame is simulated using the steady laminar flamelet chemistry. Since flamelet tables need only the

mixture-fraction PDF to obtain local density or other species values, the three simulations for this configuration evolve only the mixture-fraction PDF.

The following subsections describe the different numerical methods and the implementation in the LES solver.

Model A: DQMOM-based PDF evolution

A two-peak representation is used to evolve the mixture-fraction PDF. The delta-peak transport equations and their source terms were discussed in the previous sections. The mixing time scale for the peak-interactions is identical to the time scale used in the Lagrangian simulation. The transport equations (equations 5 and 6) are evolved using the QUICK scheme [22]. For the reactive shear layer configurations, two delta-peaks are used to describe each of the sub-filter mixture fraction and reaction progress variable PDF. The two scalars are assumed to evolve independently implying that except for the coupling through the reaction source term expression, there is no peak interaction. This simplifies the DQMOM transport equations with identical mixing and correction terms for both scalars. The reaction source term is set to zero for the mixture fraction while for the reactive scalar, the source term is evaluated at the scalar values corresponding to each environment, that is

$$S_{Y1} = S(\widetilde{Z}_1, \widetilde{Y}_1), \tag{14}$$

and

$$S_{Y2} = S(\widetilde{Z}_2, \widetilde{Y}_2), \tag{15}$$

where the subscript refers to the corresponding delta-function. The exact form of the source term is discussed later. The filtered scalar value in a given cell are obtained by a weighted summation of the delta-function locations.

$$\widetilde{Z} = w_1 \widetilde{Z}_1 + w_2 \widetilde{Z}_2, \tag{16}$$

$$\widetilde{Y} = w_1 \widetilde{Y}_1 + w_2 \widetilde{Y}_2. \tag{17}$$

For the variable density bluff-body stabilized flame, only the mixture-fraction PDF is evolved. The mean density in the computational cell is then given by

$$\bar{\rho}^{-1} = \frac{w_1}{\rho(\widetilde{Z}_1)} + \frac{w_2}{\rho(\widetilde{Z}_2)}. \tag{18}$$

The inlet conditions for the equations are based on those for the mixture fraction. It is assumed that the peaks are located at 0 and 1 at the inlet. The weight associated with each peak is determined by the mixture fraction. These boundary conditions are consistent with the assumption that the source terms $a_n = 0$. The weights then evolve according to the same equation as the mixture fraction and hence need not be solved explicitly. The wall boundary conditions for $\bar{G}_{\alpha n}$ are set identical to the boundary conditions for mixture fraction equation.

Model B: Eulerian scalar transport scheme

Here, scalar transport equations are directly solved along with the LES flow solver. For the reactive shear flow calculation, three scalars are computed. The filtered mixture fraction, second moment of the mixture fraction and the filtered reaction progress variable are solved using a finite-volume-based discretization of the scalar transport equations. The second moment of the mixture fraction is solved instead of the variance because of numerical reasons. It was

found that the production term in the variance equation was underpredicted leading to a decrease in sub-filter variance. The second moment equation, on the other hand, contains no production term but only the scalar dissipation rate that is modelled using a simple time-scale based relation.

The transport equations can be written as

$$\frac{\partial \overline{\rho}\widetilde{Z}}{\partial t} + \frac{\partial \overline{\rho}\widetilde{\mathbf{U}}\widetilde{Z}}{\partial \mathbf{x}} = \frac{\partial}{\partial \mathbf{x}}\left[(\Gamma_T + \Gamma)\frac{\partial \widetilde{Z}}{\partial \mathbf{x}}\right] \tag{19}$$

$$\frac{\partial \overline{\rho}\widetilde{Z^2}}{\partial t} + \frac{\partial \overline{\rho}\widetilde{\mathbf{U}}\widetilde{Z^2}}{\partial \mathbf{x}} = \frac{\partial}{\partial \mathbf{x}}\left[(\Gamma_T + \Gamma)\frac{\partial \widetilde{Z^2}}{\partial \mathbf{x}}\right] - \overline{\rho}\widetilde{\chi}, \tag{20}$$

$$\frac{\partial \overline{\rho}\widetilde{Y}}{\partial t} + \frac{\partial \overline{\rho}\widetilde{\mathbf{U}}\widetilde{Y}}{\partial \mathbf{x}} = \frac{\partial}{\partial \mathbf{x}}\left[(\Gamma_T + \Gamma)\frac{\partial \widetilde{Y}}{\partial \mathbf{x}}\right] + S(\widetilde{Y}), \tag{21}$$

where the scalar dissipation rate is given by

$$\widetilde{\chi} = \frac{2\Gamma_T}{\overline{\rho}\Delta^2}\widetilde{Z''^2}. \tag{22}$$

It is assumed that the sub-filter PDF for the reactive scalar is a delta-function implying that the sub-filter fluctuations of the progress variable are neglected. In this context, the DQMOM scheme will provide a higher order closure by approximating the sub-filter fluctuations by a two-peak delta-function. The scalar transport equations are solved simultaneously with the LES flow field solver using the QUICK scheme. The sub-filter mixture fraction variance can then be computed as

$$\widetilde{Z''^2} = \widetilde{Z^2} - \widetilde{Z}^2 \tag{23}$$

For the variable density simulation, the filtered mean density can then be calculated using the moments of the mixture fraction and using a beta-function as the presumed shape of the mixture-fraction sub-filter PDF:

$$\overline{\rho}^{-1} = \int \frac{1}{\rho(Z)} P(\widetilde{Z}, \widetilde{Z''^2}) dZ, \tag{24}$$

where $P(\widetilde{Z}, \widetilde{Z''^2})$ is the beta-function.

Model C: Lagrangian PDF evolution

Instead of presuming the shape of the PDF, a Monte Carlo scheme is used to evolve the PDF transport equation. Here, the fluid is represented through a statistical ensemble of particles. Each computational cell is seeded with 15 notional particles that carry a weight proportional to local cell mass. The particles are advanced in time using the time-step specified for the LES solver. In the context of hybrid methods, this is referred as a tightly coupled scheme [23]. The particles move in physical space according to:

$$d\mathbf{x}^* = \left[\widetilde{\mathbf{U}} + \frac{1}{\overline{\rho}}\nabla(\Gamma + \Gamma_T)\right]dt + \sqrt{\frac{2(\Gamma + \Gamma_T)}{\overline{\rho}}}d\mathbf{W}, \tag{25}$$

where $\mathbf{x}^*$ is the particle location and $d\mathbf{W}$ is the three-dimensional Wiener diffusion process. Due to the cylindrical coordinate frame used here, certain modification must be made. First, the velocity components corresponding to the drift term are interpolated to the particle locations using a trilinear interpolation scheme. Then, the drift term is converted to a Cartesian reference

frame using geometrical transformation. The diffusion component is added to the adjusted drift term and the particle velocity converted back to the cylindrical reference frame. Particles are then tracked in the computational domain using a face-to-face strategy [13]. Also, a parallel domain decomposition identical to the LES decomposition is used to speed up the computation. Further details of the Lagrangian scheme are described elsewhere [24].

Transport in composition space is split into molecular mixing and reaction sub-steps. To be consistent with the DQMOM scheme, the IEM model [20] is used to describe mixing. The micromixing sub-step can then be written as

$$d\phi^* = \frac{\chi}{2\widetilde{Z''^2}}(\widetilde{\phi} - \phi^*)dt, \tag{26}$$

where ϕ^* is the composition vector $[Z^*\ Y^*]$ of a single notional particle. The mixing time scale is identical for both scalars. The reaction progress variable is then advanced in time according to a reaction sub-step.

$$dY^* = S(Z^*, Y^*)dt. \tag{27}$$

For the reacting shear flow simulation, both the mixture fraction and the reaction progress variable are used. The filtered scalar values in a computational cell is given by

$$\widetilde{\phi} = \sum_{i=1}^{i=N} w_i \phi_i^*, \tag{28}$$

where N is the number particles in a given cell. For the bluff-body flame simulation, only the mixture fraction is evolved. The mean density in each computational cell is determined using the particles in that particular cell. Using the particles weights, the mean property at the $(t + dt)$ iteration can be obtained as:

$$\overline{\rho}^{-1} = \sum_{i=1}^{N} \frac{w_i}{\rho(Z_i)}, \tag{29}$$

where $\rho(Z)$ is obtained from the flamelet solution. It is evident that any non-linear property based on the mixture fraction can be obtained using the above equation. The temperature profiles shown in the comparisons below are obtained using a similar summation.

4. Numerical tests

This section compares the DQMOM approximation against standard techniques available for reactive flow simulations.

4.1 *Reactive shear layer simulations*

The shear flow geometry of Mungal *et al.* [25] is used to test the new scheme. The configuration consists of a planar shear layer formed by two streams entering with bulk velocities of 8.8 m/s and 22 m/s, respectively. Although the experiment involves low heat-release fast chemistry, in this work we have not implemented this mechanism. Since the purpose is to compare different reaction models, a simple first order mechanism of the type $A + B \rightarrow P$ is used for modelling reaction. The rate expression is simplified using a mixture fraction-progress variable approach. Three different rate expressions that commonly occur in reacting flows are tested. The transported PDF scheme is also simulated for the same flow conditions and the results are compared with the DQMOM and LES simulations. A 256×128 grid spanning

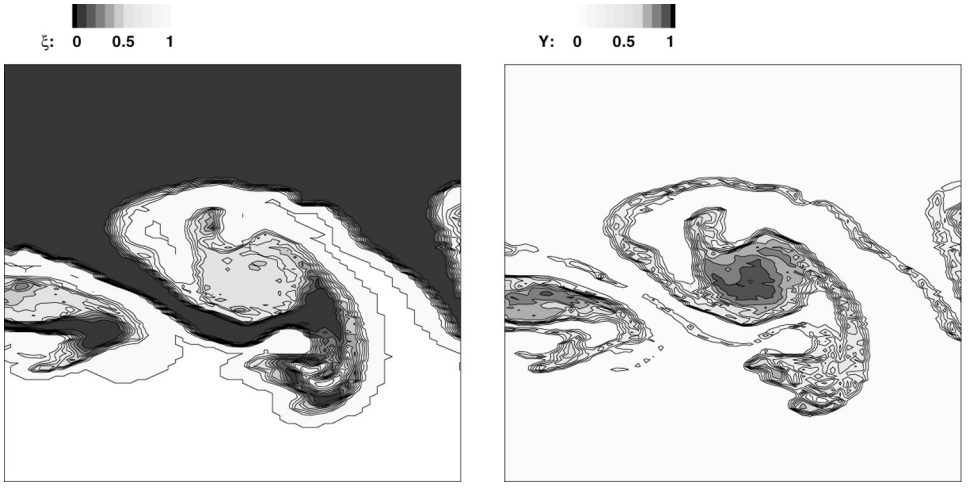

Figure 2. Instantaneous mixture fraction (left) and progress variable (right) contours simulated using the FDF scheme.

$80D$ in the axial direction and $40D$ in the cross-stream direction is used. D is set arbitrarily to 1 cm. The inlet velocity profiles are assumed to be laminar with flat profiles. A development region corresponding to $10D$ extends into the domain where the two streams are separated by a splitter plate.

In all the simulations, the rate expression for the progress variable is of the form

$$r_Y = K\left(\frac{Z}{Z_{st}} - Y\right)\left(\frac{1-Z}{1-Z_{st}} - Y\right). \tag{30}$$

The rate constant K is varied to study the effect of non-linearity on DQMOM predictions. In the first case, the rate constant is set to a value of $K = 2$. Figure 2 shows the instantaneous mixture fraction and progress variable contours near the centre of the domain. It shows the vortex like structure common to shear flows and the presence of highly mixed reactants at the centre of such vortices. The peak in source term and mean progress variable are observed near the centreline. The vortices were found to stretch to a maximum of 10D in the cross-stream direction. It was found that the DQMOM model exhibits similar high reaction-rate zones. However, the LES simulations using the Eulerian transport equations (Model B) show a thick reaction zone with maximum allowable reaction rate at each location. In order to compare the steady-state trends, mean and variance of all scalars were time-averaged for at least one flow through time. Figure 3 shows the cross-stream profiles of the mixture fraction and sub-grid variance computed from all three schemes. Theoretically, the sub-grid variance obtained from all these methods should be identical. However, the differences in the implementation cause some discrepancy. Nevertheless, the time-averaged filtered mixture fraction and sub-grid variance predicted by all the schemes are in good agreement, thereby validating both the DQMOM and transported-PDF implementation.

The time-averaged mean and sub-grid variance of the reaction progress-variable obtained from the different schemes show some interesting features (figure 4). The sub-grid variance is non-zero only for the DQMOM and transported-PDF schemes and is zero for the Eulerian scheme (Model B). In this context the LES solver can be considered as a one-peak DQMOM model with complete sub-filter mixing. If the transported-PDF scheme is considered as a

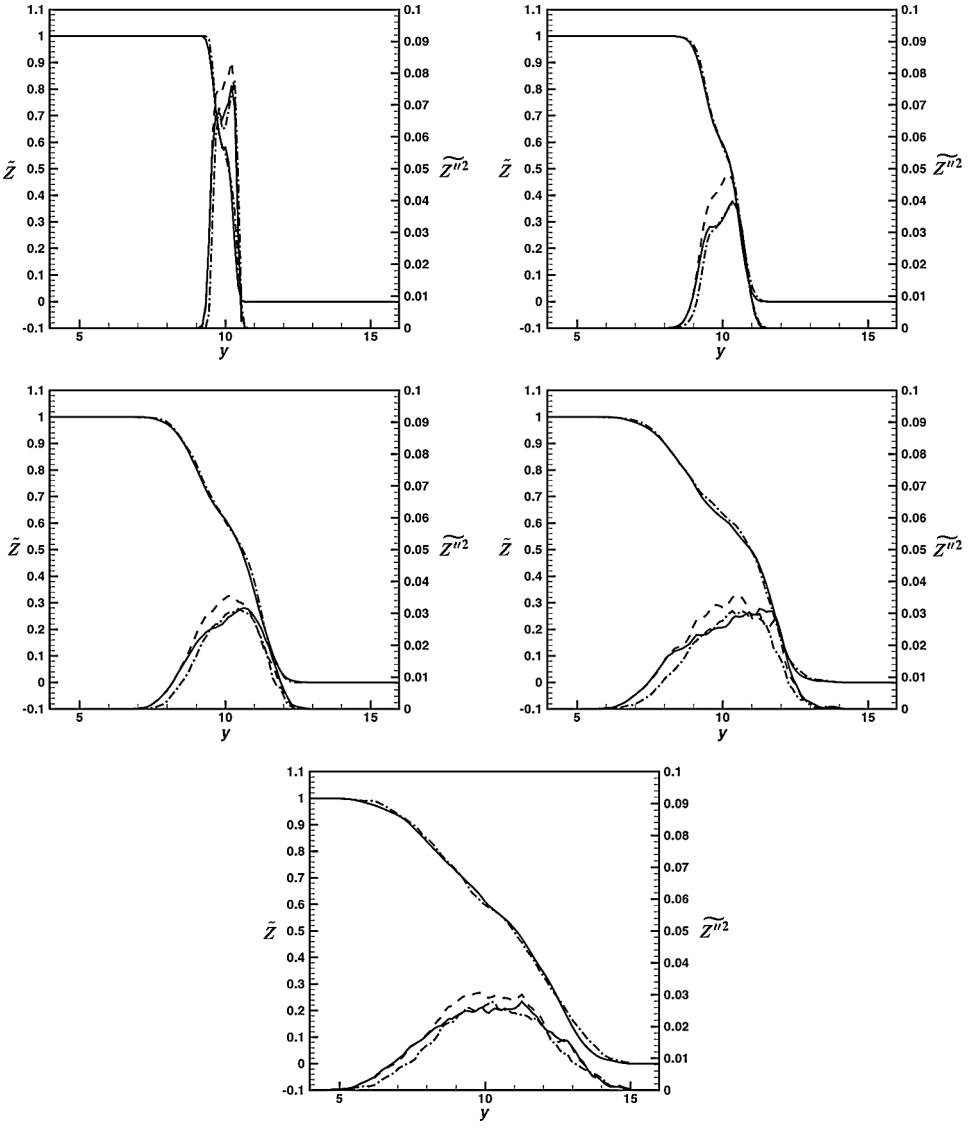

Figure 3. Comparison of time-averaged mean and variance of mixture fraction at different axial locations. (—) DQMOM scheme, (– – – –) Eulerian transport scheme, and (— – —) Lagrangian-FDF scheme.

multi-environment DQMOM model, the particle scheme with a nominal number density of N represents an N-environment decomposition of the FDF. The cross stream profiles of the mean show that the DQMOM method provides a vast improvement over the one-environment solution. The mean profile shows that in spite of the simple rate expression, second moment terms cannot be neglected. The differences between the LES (Model B) and DQMOM models are highest in the initial section where the effect of unmixed reactants will be very important. Since the inflow is laminar, the mixing layer itself does not become turbulent until about $X = 7.5$. However, the Eulerian solver predicts very high reaction rates in even these laminar regions where low mixing should essentially keep the reaction rates to a very low value. This 'early-ignition' is observed in the profiles at $X = 20$ where the mean value predicted by the

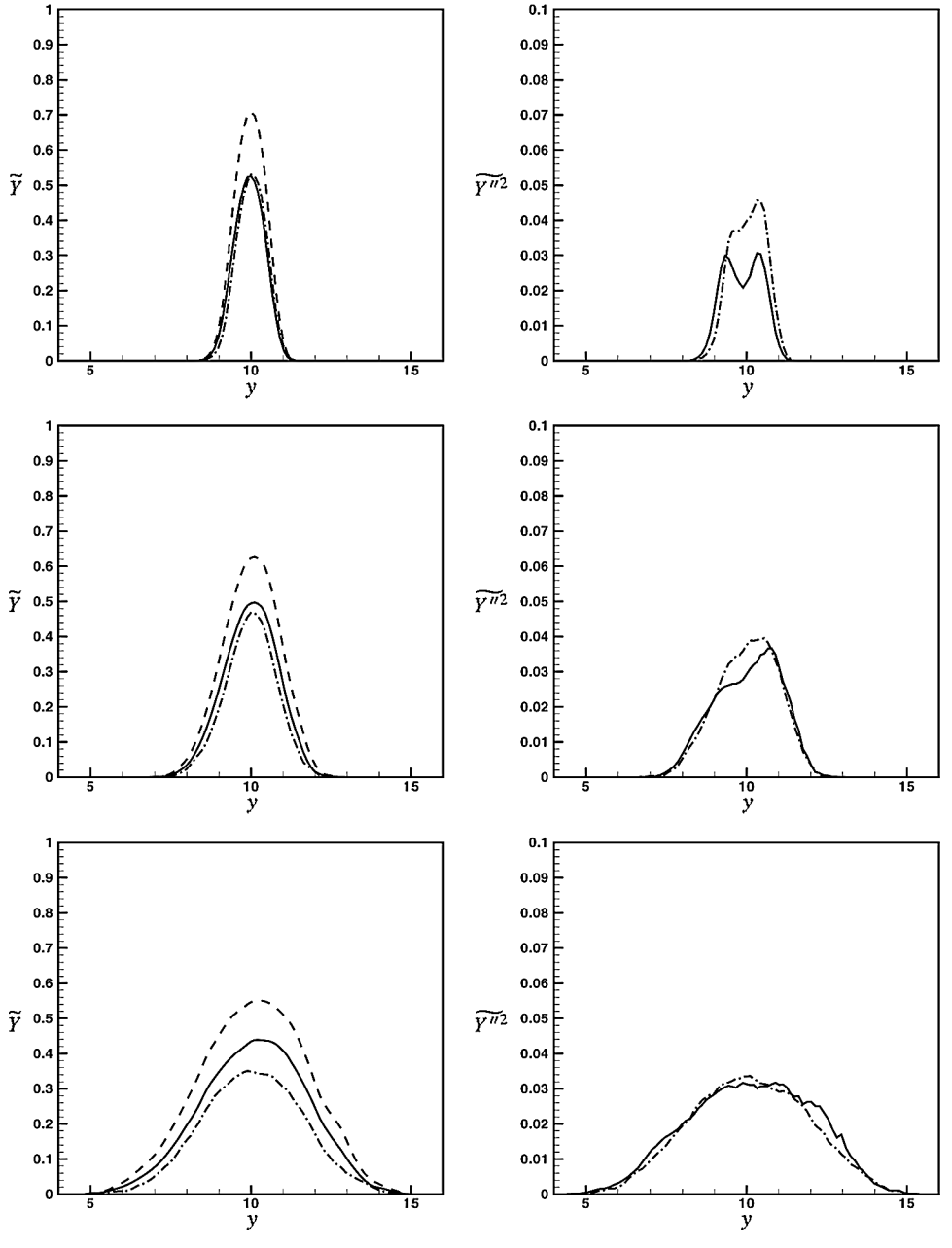

Figure 4. Comparison of time-averaged (left) mean and (right) variance of reaction progress variable using a constant rate constant at (top) $X = 20$, (middle) $X = 30$ and (bottom) $X = 50$. (———) DQMOM scheme, (– – – –) Eulerian LES scheme, and (— – —) Lagrangian-FDF scheme.

LES solver (Model B) is at least 50% higher than that predicted by the DQMOM model. Surprisingly, the sub-grid variance profile from the DQMOM scheme also shows very good agreement with the PDF scheme. This essentially implies that the third and higher moments of the reactive scalar can be neglected for this chemistry scheme.

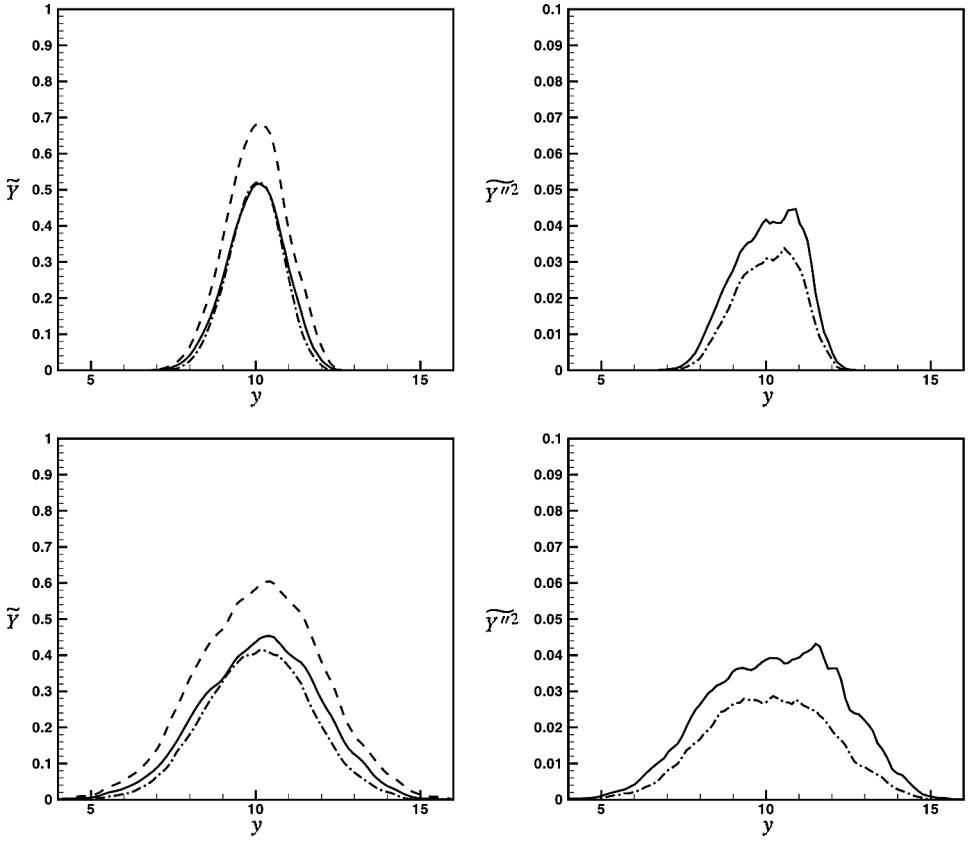

Figure 5. Comparison of time-averaged (left) mean and (right) variance of reaction progress variable for exponential reaction rate at (top) $X = 30$ and (bottom) $X = 50$. (———) DQMOM scheme, (– – – –) Eulerian-LES scheme, and (— – —) Lagrangian-FDF scheme.

In the next case, a more complex rate expression is implemented. Reaction rates appearing in combustion have a strong dependence on temperature. Most source terms have an exponential dependence on local temperature. To simulate such a condition, the reaction rate constant was set to

$$K = 1000 \exp\left(-\frac{b(1-Y)}{1-0.88(1-Y)}\right), \tag{31}$$

where b denotes the degree of dependence on temperature. For practical combustion applications, b is usually set to values between 5 and 6. However, such high values lead to extinction for the present flow configuration. Instead, a lower value of 1 is chosen so that the reaction zone can be anchored near the splitter plate. This implies a weaker dependence on temperature but nevertheless makes the rate expression non-linear. Figure 5 shows the cross-stream profiles of reaction progress variable. Here again, it can be seen that the DQMOM predictions of both the mean and the variance of the reactive scalar are in good agreement with the transported-PDF results. The LES (Model B) predictions show fast rates consistent with the laminar assumption. It should be noted that depending on the reaction rates, the complete mixing assumption can also lead to quenching.

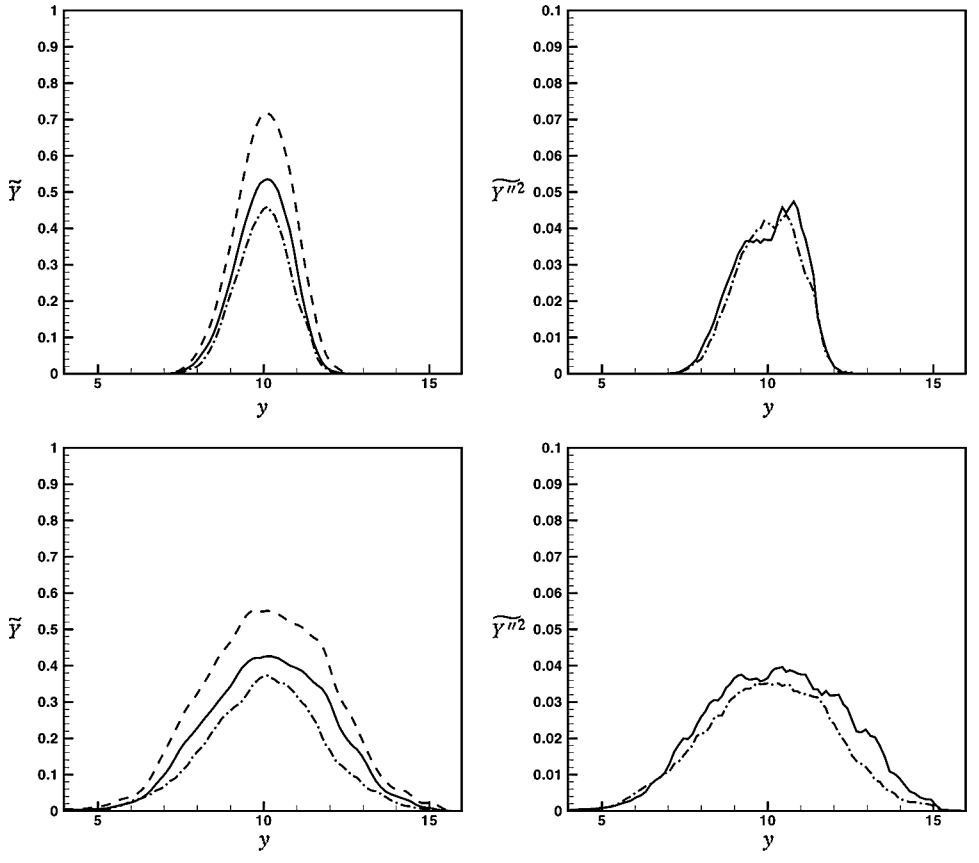

Figure 6. Comparison of time-averaged (left) mean and (right) variance of reaction progress variable for polynomial reaction rate at (top) $X = 30$ and (bottom) $X = 50$. (———) DQMOM scheme, (– – – –) Eulerian LES scheme, and (— – —) Lagrangian FDF scheme.

The third and final case uses a polynomial rate function which is common to chemical engineering assumptions. Reduced chemical mechanisms like the chloromethane reactions [26] may even involve non-integer moments of the scalar variable. Here, the rate is defined as

$$r_Y = 1000\frac{0.0001 + Y^2}{1.0 + Y}. \tag{32}$$

This expression ensures that the reaction proceeds without the need for an ignition source. The predicted mean and variance (figure 6) indicate good agreement with the transported-PDF scheme. This clearly shows that the DQMOM model with just two environments is able to drastically improve the results obtained by neglecting sub-filter scalar fluctuations (Model B).

In terms of computational requirements, the particle-based transported-PDF solver is nearly five times slower than the DQMOM scheme, even for such simple geometries. For complex configurations, the memory requirements of a large ensemble of particles can further slow down the simulation. However, the DQMOM scheme it not without limitations. In particular, detailed chemistry mechanisms will require a large number of scalar transport equations and may eventually diminish the advantages over the particle scheme. In spite of these limitations which are common to all explicit time-stepping algorithms, the present study shows that the

DQMOM scheme is a viable alternative to the Monte Carlo based transported-PDF model and needs to be further explored for multispecies systems.

4.2 *Bluff-body stabilized flame simulations*

The bluff-body stabilized flame is used as a test case for studying the feasibility and accuracy of the DQMOM scheme. It is known that simple chemistry models like the laminar flamelet model can reproduce the species profiles quite accurately for this flame [27]. Hence, we use the laminar flamelet chemistry model for the simulations performed here. The primary objective of the simulations is to evolve the mixture-fraction PDF. Since the mixture-fraction equation contains no reaction source terms, all the models should evolve the same equations. However, the sub-filter mixture-fraction PDF will determine the density field which influences the flow field. For the Eulerian scalar scheme (Model B), the beta-function approximation will be used. The Lagrangian scheme will evolve the sub-filter PDF through the particle equations. If the DQMOM scheme is a viable method, it should be able to match the predictions of both the beta-function based scalar model and the Lagrangian model.

One other aspect to note is that in this test case, the flow field and the scalar field are coupled through the density field. Variable density flows are inherently challenging to simulate due to the feedback of the density field from the scalars. One of the main drawbacks of the Lagrangian-particle based hybrid simulation is that the filtered-density fields computed from the particle composition contains stochastic noise. This makes the feedback numerically unstable and can lead to unbounded increase in the error. The DQMOM method, on the other hand, is deterministic and will not introduce stochastic errors. The low-Mach number formulation used here is known to be stable for reasonably large density changes that usually occur in combusting flows. However, the rate of change of density is an important parameter that controls stability. Here, the three different simulation strategies are used to compute a bluff-body stabilized flame. It was found that the Lagrangian scheme requires special modifications in-order to obtain convergence. The exact nature of the modifications are beyond the scope of the present discussion and details of the scheme are provided elsewhere [24].

The computational setup corresponds to the experiments performed at the University of Sydney [16]. The fuel mixture consisting of a 1:1 volumetric ratio of methane and hydrogen issues through a central jet of 3.6 mm diameter at a bulk velocity of 108 m/s. The coflow of air at 35 m/s is separated from the fuel jet by an annular bluff-body of 50 mm diameter. All simulations are carried out on a $320 \times 120 \times 64$ grid in a cylindrical coordinate frame. The domain spans 100 D in the axial direction and 20 D in the radial direction where D is the diameter of the fuel jet (figure 7). A structured flow solver with dynamic Smagorinsky models for turbulent viscosity and turbulent diffusivity is used [28]. The inlet conditions for the central jet are obtained from a precomputed LES of a periodic turbulent pipe flow. The coflow is assumed to have a 1/7 power law profile for the axial velocity component and zero radial and azimuthal velocity components. The flamelet library is computed using a single strain rate of 100 s^{-1} from GRI-2.11 chemistry mechanism. It has been shown elsewhere [27] that even such a simple representation is sufficient to capture the dynamics of this system.

For the Lagrangian particle scheme, the computational domain was uniformly seeded with 15 particles per computational cell. The particle weights were normalized based on an arbitrary scale such that the sum of the particle weights in each cell was proportional to the cell mass. Both the Lagrangian and DQMOM simulations were started from a statistically stationary beta-PDF based simulation. Then all the simulations were run for approximately 2.5 residence times calculated based on the inlet coflow bulk velocity and the length of the domain. Time-averaging was then started and continued for 1.5 residence times. It was found that longer

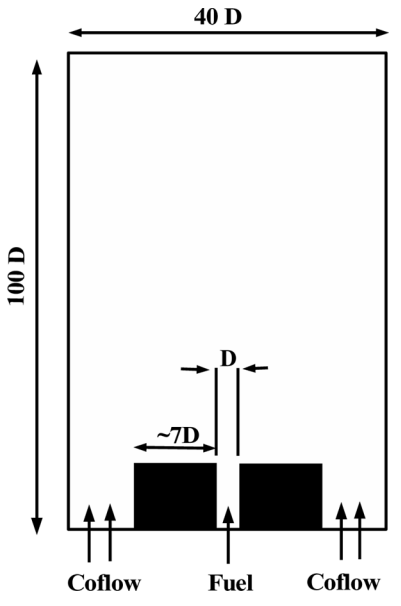

Figure 7. Computational domain used for the bluff-body stabilized flame simulation.

time averaging did not change the mean profiles. All simulations were performed using MPI based domain decomposition and utilized 32–48 processors. It was found that the Lagrangian scheme was 12 times slower and the DQMOM scheme was 1.8 times slower compared to the beta-PDF scheme. The results of the simulation are discussed next.

Figure 8 shows the salient features of the bluff body flow. The presence of the solid body induces a recirculation zone that tends to increase the extent of the reaction zone. In addition, the large-scale recirculation also leads to a near uniform highly mixed region near the bluff-body. This high-temperature region and the resulting counter-rotating vortex like structures lead to a stable flame. It should be noted that in the absence of this recirculation region, the reaction zone will be located far downstream leading to a lifted flame structure. At these high Reynolds number flows, such a lifted configuration will ultimately lead to flame blowout. The counter-rotating core region helps to mix the initially segregated fuel and oxidizer. The lean stoichiometric value of the fuel mixture leads to a high temperature region in the secondary shear layer between the recirculating flow over the bluff-body and the coflow. This favorable

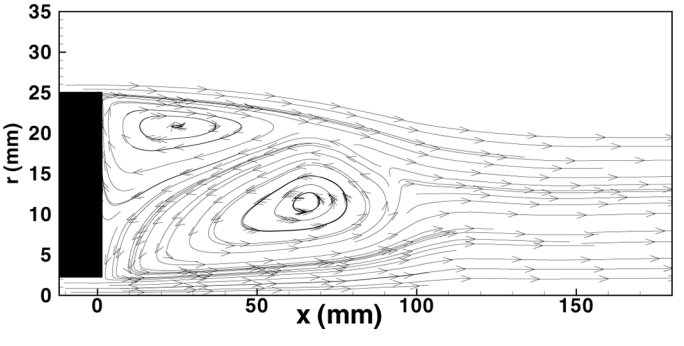

Figure 8. Streamline trace near the bluff-body illustrating the presence of recirculation regions.

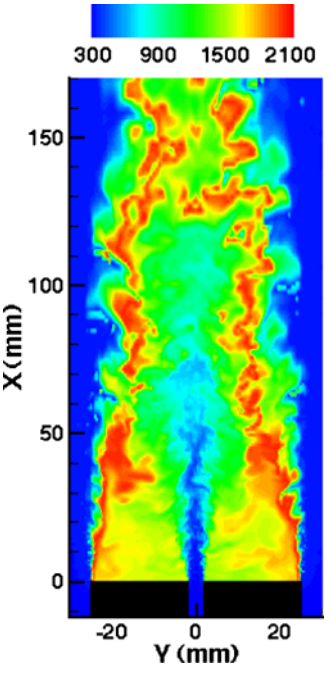

Figure 9. Instantaneous temperature field showing the complex flow patters in the configuration. The blue region marks 294 K and the red region marks 2000 K. Maximum temperature in the domain is 2089 K.

mixing leads to large energy release that is then carried inward into the primary shear layer where the fuel interacts with burnt gases. It is evident that both these shear layers are associated with steep temperature and density gradients and hence a well-resolved grid structure is essential for good predictions and general algorithmic stability.

Figure 9 shows a contour plot of the instantaneous temperature that clearly indicates a uniform temperature zone near the bluff body. Downstream of the bluff-body, a secondary reaction zone is formed where pre-heated fuel mixes with coflow leading to high temperatures characteristic of the recirculation zone. However, the small volume of the fuel compared to the coflow causes dilution of enthalpy leading to reduced temperatures further downstream. In spite of the apparent uniformity of the recirculation zone, local dynamic events occur periodically to refresh the fluid entrapped in this low velocity region. The outer shear layer is characterized by rolling vortices that are formed at the edge of the bluff-body. These Kelvin–Helmoltz type instabilities lead to enhanced mixing near the stoichiometric surface and leads to reduced time-averaged temperatures.

Figures 10 and 11 show comparisons of flow-field quantities with experimental data. Time-averaged radial profiles of mean axial velocity, radial velocity and RMS axial velocity are presented at two different axial locations. The plots only compare results from the DQMOM simulation. It was found that neither the beta-PDF or Lagrangian scheme showed significant variation and hence this discussion is omitted here. It is seen that the LES computation is able to predict all components of the flow field reasonably accurately. Similar agreement was found at other axial stations both close to the bluff-body and at downstream zones and has been omitted. It is emphasized that to improve predictions, a more sophisticated simulation methodology is required. Here the filter-size and the mesh are varied in-order to satisfy a set of resolution constraints. Simulation results based on this optimization procedure are found to yield very good comparison with experiments [27]. For the present study, the focus is

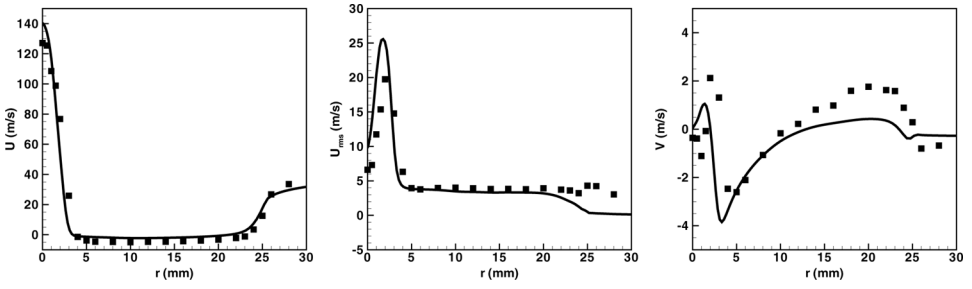

Figure 10. Comparison of time-averaged radial profiles of axial velocity (left), RMS axial velocity (middle) and radial velocity (right) at an axial location of $x = 10$ mm. Symbols denote experimental data and lines show simulation results obtained using the DQMOM scheme.

on analyzing the feasibility of the DQMOM scheme. Hence we limit the discussion to the simulations carried out with a fixed grid.

Figure 12 compares time-averaged temperature profiles at different axial locations. In general, all the simulations compare well with experimental data at all axial locations considered. However, certain distinct trends are noticed. The DQMOM scheme closely reproduces the beta-PDF results at locations close to the bluff-body. At $x = 13$ mm, the Eulerian simulations predict a peak in temperature in the shear layer formed by the coflow and the recirculating burnt gases ($r \approx 25$ mm). However, the Lagrangian scheme accurately reproduces the experimentally observed drop in temperature. The inherent numerical diffusion in the Eulerian scheme can lead to reduction in sub-filter variance that results in an increase in local temperature. This effect seems to be more pronounced when the mixture fraction values are close to zero where the non-linearities in the flamelet profiles are dominating. At successive downstream locations, the peaks in the temperature appear less pronounced and at $x = 90$ mm, the differences are small.

In spite of using a simple approximation, the DQMOM scheme is able to predict the mean temperature profiles quite accurately. Since large-eddy simulations resolve the large-scale structures, the sub-filter component is usually small compared to the resolved scales. Thus the sub-filter PDF can be expected to have a narrow spread in composition space. Clearly, a two-peak approximation is sufficient to describe sub-filter PDF in such situations. Locally, large sub-filter variance (as a fraction of the intensity of segregation, $Z(1 - Z)$) is observed, although such variations are usually confined to the shear regions near the edge of the bluff-body. Simulations that use no sub-filter model led to higher temperatures in the recirculation

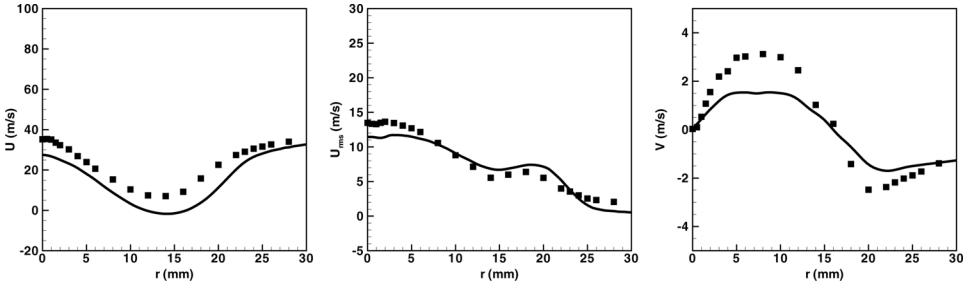

Figure 11. Comparison of time-averaged radial profiles of axial velocity (left), RMS axial velocity (middle) and radial velocity (right) at an axial location of $x = 90$ mm. Symbols denote experimental data and lines show simulation results obtained using the DQMOM model.

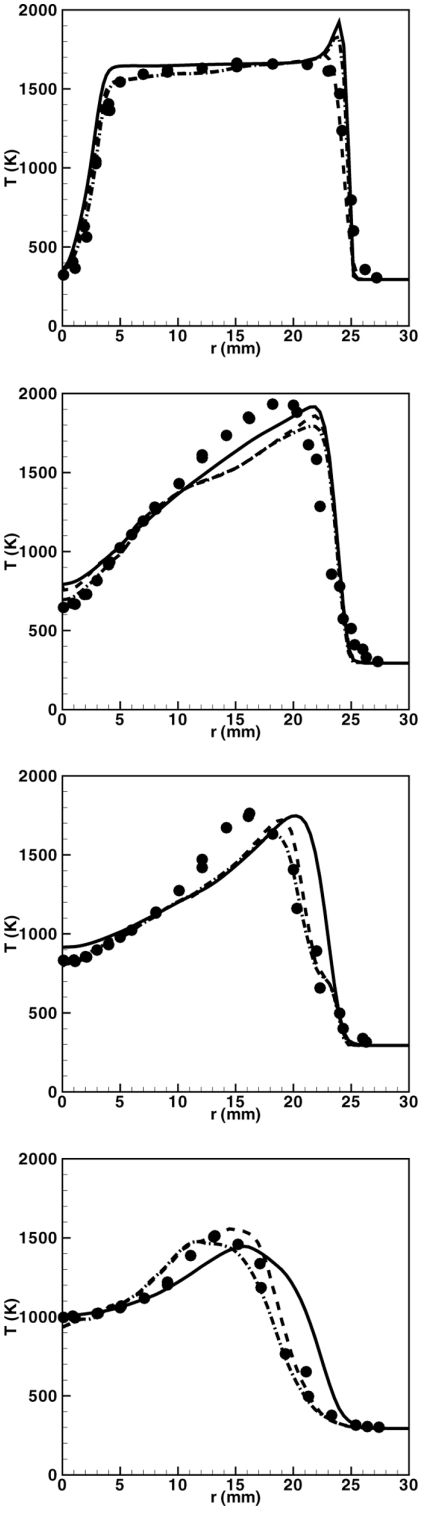

Figure 12. Comparison of time-averaged radial temperature profiles at different axial locations. Solid lines show DQMOM results, dashed lines show PDF results, and dashed-dotted lines show beta-PDF results. Symbols denote experimental data. From top to bottom, at axial locations of $x = 13$, 45, 65, and 90 mm.

region that was at least 200 K higher than that predicted in the simulations that use a sub-filter model.

5. Conclusions

The DQMOM model was formulated for large-eddy simulation and applied using a structured LES solver for both constant and variable density flows. A bluff-body stabilized flame as well as a reactive shear layer were simulated using the DQMOM sub-filter model as well as a conventional Lagrangian scheme. In addition, Eulerian transport equations for the filtered mean and variance of the mixture fraction as well as the reactive scalar are also solved. Using a simple shear-flow configuration, the feasibility and accuracy of a two-peak DQMOM scheme was established. It was shown that the DQMOM scheme provides comparable accuracy to a Monte Carlo based Lagrangian scheme for a two-scalar chemistry with different rate expressions. At the same time, the DQMOM scheme is computationally cheap and can be readily implemented in existing LES solvers. Further, the DQMOM scheme was implemented in a variable-density formulation of the LES solver and used to compute a complex bluff-body stabilized flame. Comparison of time-averaged profiles show that all three schemes predict the experimental data quite accurately. In spite of the simplified representation of the PDF in the DQMOM model, the temperature profiles were found to agree well with beta-PDF and Lagrangian schemes.

The DQMOM formulation allows a natural extension to multiple reactive scalars. However, it should be noted that with increase in the number of scalars, the computational cost will increase too. Future work will involve simulation aimed at understanding the scaling of computational cost based on the needs of specific applications. DQMOM has applications not only in combustion but in the discretization of any PDF evolution equation. One recent application [29] uses DQMOM to discretize the conditional PDF transport equation. This provides a natural approach to formulating higher-order conditional moment closure schemes. It is clear that the DQMOM scheme has a wide-range of applicability in turbulent reactive flow modelling. Future efforts will involve extensions to more detailed chemistry schemes and to understand the effect of the number of delta-peaks on the accuracy and cost of the simulations.

References

[1] Colucci, P.J., Jaberi, F.A. and Givi, P., 1998, Filtered density function for large eddy simulation of turbulent reacting flows. *Physics of Fluids*, **10**, 499–515.

[2] Pope, S.B., 1985, PDF methods for turbulent reactive flows. *Progress in Energy and Combustion Science*, **11**, 119–192.

[3] Peters, N., 2000, *Turbulent Combustion* (Cambridge: Cambridge University Press).

[4] Bilger, R.W., 1993, Conditional moment closure for turbulent reacting flow. *Physics of Fluids*, **5**, 436–444.

[5] Cook, A.W. and Riley, J.J., 1994, A subgrid model for equilibrium chemistry in turbulent flows. *Physics of Fluids*, **10**, 499–515.

[6] Jimenez, J., Linan, A., Rogers, M.M. and Higuera, F.J., 1997, *A priori* testing of subgrid models for chemically reacting non-premixed turbulent flows. *Journal of Fluid Mechanics*, **349**, 149–171.

[7] Wall, C., Boersma, B. and Moin, P., 2000, An evaluation of the assumed beta probability density function subgrid scale model for large eddy simulation of non-premixed turbulent combustion with heat release. *Physics of Fluids*, **7**, 2522–2529.

[8] Mellado, J.P., Sarkar, S. and Pantano, C., 2003, Reconstruction subgrid models for nonpremixed combustion. *Physics of Fluids*, **15**, 3280–3307.

[9] Pope, S.B., 1981, A Monte Carlo method for the PDF equations of turbulent reactive flow. *Combustion Science and Technology*, **25**, 159–174.

[10] Jaberi, F.A., Colucci, P.J., James, S., Givi, P. and Pope, S.B., 1999, Filtered mass density function for large-eddy simulation of turbulent reacting flows. *Journal of Fluid Mechanics*, **401**, 85–121.

[11] Masri, A.R. and Pope, S.B., 1990, PDF calculations of piloted turbulent nonpremixed flames of methane. *Combustion and Flame*, **81**, 13–29.

[12] Muradoglu, M., Jenny, P., Pope, S.B. and Caughey, D.A., 1999, A consistent hybrid finite-volume/particle method for the PDF equations of turbulent reactive flows. *Journal of Computational Physics*, **154**, 342–371.
[13] Raman, V., Fox, R.O. and Harvey, A.D., 2004, Hybrid finite-volume/transported PDF simulations of a partially premixed methane–air flame. *Combustion and Flame*, **136**, 327–350.
[14] Fox, R.O., 2003, *Computational Models for Turbulent Reacting Flows* (Cambridge: Cambridge University Press).
[15] Marchisio, D.L. and Fox, R.O., 2005, Solution of population balance equations using the direct quadrature method of moments. *Journal of Aerosol Science*, **36**, 43–73.
[16] Dally, B.B., Masri, A.R., Barlow, R.S. and Fietchner, G.J., 1998, Instantaneous and mean compositional structure of bluff-body stabilized nonpremixed flames. *Combustion and Flame*, **114**, 119–148.
[17] Muradoglu, M., Liu, K. and Pope, S.B., 2003, PDF modeling of a bluff-body stabilized turbulent flame. *Combustion and Flame*, **132**, 115–137.
[18] Dally, B.B., Fletcher, D.F. and Masri, A.R., 1998, Flow and mixing fields of turbulent bluff-body jets and flames. *Combustion Theory and Modelling*, **2**, 193–219.
[19] Kim, S.H. and Huh, K.Y., 2002, Use of conditional moment closure model to predict NO formation in a turbulent CH_4/H_2 flame over a bluff-body. *Combustion and Flame*, **130**, 94–111.
[20] Villermaux, J. and Falk, L., 1994, A generalized mixing model for initial contacting of reactive fluids. *Chemical Engineering Science*, **49**, 5127–5140.
[21] Wang, L. and Fox, R.O., 2004, Comparison of micromixing models for CFD simulation of nanoparticle formation by reactive precipitation. *AIChE Journal*, **50**, 2217–2232.
[22] Leonard, B.P., 1979, A stable and accurate convective modelling procedure based on quadratic upstream interpolation. *Computational Methods in Applied Mechanics*, **19**, 59–98.
[23] Jenny, P., Pope, S.B., Muradoglu, M. and Caughey, D.A., 2001, A hybrid algorithm for the joint PDF equation of turbulent reactive flows. *Journal of Computational Physics*, **166**, 218–252.
[24] Raman, V., Pitsch, H. and Fox, R.O., 2005, A consistent hybrid LES-FDF scheme for the simulation of turbulent reactive flows. *Combustion and Flame*, **143**, 56–78.
[25] Mungal, M. and Dimotakis, P.E., 1984, Mixing and combustion with low heat release in a turbulent mixing layer. *Journal of Fluid Mechanics*, **148**, 349–382.
[26] West, D.H., Hebert, L.A. and Pividal, K.A., 1999, Detection of quenching and instability in industrial chlorination reactors, in: *Fall AIChE Annual Meeting*, Dallas, 1999.
[27] Raman, V. and Pitsch, H., 2005, Large-eddy simulation of bluff-body stabilized non-premixed flame using a recursive-refinement procedure. *Combustion and Flame*, **142**, 329–347.
[28] Pierce, C.D., 2001, Progress-variable approach for large-eddy simulation of turbulence combustion. PhD thesis, Stanford University.
[29] Fox, R.O. and Raman, V., 2004, A multienvironment conditional probability density function model for turbulent reacting flows. *Physics of Fluids*, **16**, 4551–4565.